An Analysis of Satellite Infrared Soundings at the Mesoscale Using Statistical Structure and Correlation Functions

DONALD W. HILLGER AND THOMAS H. VONDER HAAR

Department of Atmospheric Science, Colorado State University, Fort Collins 80523

(Manuscript received 22 March 1978, in final form 1 November 1978)

ABSTRACT

A statistical analysis of satellite infrared sounding data from the Vertical Temperature Profile Radiometer (VTPR) on NOAA 4 was performed in conjunction with the National Severe Storms Laboratory (NSSL) mesoscale sounding period (10 May–12 June 1976). Satellite radiances, retrieved temperatures and moisture information in the form of radiance residuals at a resolution of ~70 km were examined for a 14-day composite period using structure and correlation functions. A structure analysis as a function of data separation distance for a field of measured values can detect the mean nondirectional gradient in the field. Estimates of the relative noise level in the measurements were also obtained by extrapolating the obtained structure to zero separation distance. The rms radiance noise levels for the VTPR channels were found to be close to the design specifications for the VTPR instrument. For retrieved temperatures, the noise level was determined to be ~0.5°C at the three pressure levels examined.

The structure functions for all available satellite-derived temperatures in the composite period compared favorably to similar results computed using high-resolution NSSL rawinsonde data. However, moisture correlation results demonstrated that the satellite-derived moisture in the integrated sense is not an equivalent substitute for mesoscale rawinsonde soundings. The structure-function analysis was also applied to each of the 14 individual days of available satellite data. The structure as a function of distance for VTPR channels 6 and 7 reflect mainly lower tropospheric temperature and moisture gradients, respectively. On days with both large temperature and moisture gradients as detected by the satellite these gradients appeared to be associated with severe storms later in the day. A structure-function analysis of satellite-derived 500 mb temperature fields was also found to detect existing upper air patterns on individual days.

The information content of individual temperature and moisture fields derived from the satellite soundings was interpreted by comparison with similar fields from conventional rawinsonde soundings. Fields of both temperature and moisture from the two instruments were compared by direct correlation of the two sets of measurements. Discrepancies existed between the compared fields, but they were to a large extent explained by differences between the two measuring systems and time and space scale differences between the measurements. According to the analysis, temperatures were retrieved from the satellite data with reasonable success on most of the days at both 300 and 500 mb, but with much less success at 700 mb. Again, the moisture information extracted from the satellite data was not as promising due to its integrated effect and due to the small observed moisture gradients on some days.

Structure-function analysis of satellite temperature soundings was shown to provide a means of interpreting these satellite data. It demonstrated that high-resolution satellite soundings provide information about spatial variations of temperature structure equivalent to that provided by high-density rawinsondes.

1. Introduction

There is an increasing need for high-resolution temperature and moisture information. Programs such as the Severe Environmental Storms and Mesoscale Experiment (SESAME) (Lilly, 1975) have been proposed to quantitatively test new techniques for observation and analysis of mesoscale phenomena. Also, an increase in the quantitative understanding of the interaction of various space scales, from that of convective storms to the larger scale environment, will probably only be a result of increased resolution data. Such mesoscale information, on the meso-β scale (25–250 km) and larger, should be readily available from satellite measurements. Satellites also have the ability to supply the large amount of temperature and moisture information required by computer simulation models. However, this will only become true if the data can be correctly utilized. Tracton aud McPherson (1977) have shown a null impact for using satellite data on NMC operational numerical weather prediction in the Northern Hemisphere when the satellite data are used at the scale of rawinsonde soundings (~400 km). However, a positive impact has been shown by using high-resolution Nimbus 6 sounding data in Australian region forecasts (Kelly *et al.*, 1978). Others have shown a similar positive impact for satellite sounding information on 500 mb analyses when care is taken to screen the data (Petersen and Horn, 1977).

0022-4928/79/020287-19$08.75

TABLE 1. NOAA VTPR channels.

Channel no.	Wavelength (μm)	Wavenumber (cm^{-1})	Approximate peak level of weighting function (mb)
CO_2 channels: 15 μm CO_2 absorption band			
1 (Q branch)	14.96	668.5	30
2	14.77	677.5	50
3	14.38	695.0	120
4	14.12	708.0	400
5	13.79	725.0	600
6	13.38	747.0	surface
H_2O channel: Rotational water vapor absorption band			
7	18.69	535.0	700
Window channel: Atmospheric window region			
8	11.97	833.0	surface

The full impact will only be realized if the satellite data are used on small space and time scales, such as from geosynchronous orbit where its advantages may become apparent. Both mesoscale forecasting for field experiments and mesoscale computer models will be the real test of satellite sounding capabilities (Kreitzberg, 1976).

The present statistical analysis using structure and correlation functions is intended to test the quality of present-day operational satellite sounding information on the mesoscale. Data from the Vertical Temperature Profile Radiometer (VTPR) on NOAA 4 are used at full resolution (~70 km). The structure as a function of distance for a set of high-resolution data reflects the mean nondirectional gradient in the observed field. Also, when extrapolated to zero separation distance, the structure value estimates a relative noise level or uncertainty for the data. Only with high-resolution data can this value be determined, since the measurements at the smallest separation nearly reflect the reproducibility of the measurements.

Results of the structure-function analysis on 14 days of available satellite data for the 1976 National Severe Storms Laboratory (NSSL) sounding period (10 May–12 June 1976) are compared to a similar analysis of the NSSL mesoscale rawinsonde data. The satellite data are also analyzed on a day-by-day basis in terms of calibrated radiances for each satellite pass at approximately 0900 GMT. The 14 individual days of available satellite data show an ability to detect middle-to-low-level tropospheric temperature and moisture gradients. These gradients are represented by an increase in structure with increased sounding separation distance for radiances from VTPR channels 6 and 7. Such data are independent of any conventional data sets. Days with the largest increase in structure with distance appear to have a potential for severe weather (e.g., thunderstorms, hail, funnel clouds) when compared to significant weather events, if any, later in the day. A structure-function analysis of satellite-derived 500 mb temperatures was also performed and compared to upper air features on a daily basis.

A final analysis of the individual satellite-derived temperature and moisture fields was a direct correlation with fields of conventional rawinsonde data. The result of this direct correlation analysis is another measure of the ability to retrieve information from satellite data as compared to rawinsonde data. Temperatures retrieved at three levels (300, 500 and 700 mb) and moisture information in terms of radiance residuals for the VTPR H_2O channel were examined at the mesoscale. It is noted that higher resolution and quality satellite sounding data are anticipated from third generation sounders such as Nimbus 6 (1975–76) and a similar instrument to be launched on TIROS-N in 1978 for operational use.

2. Satellite soundings and area of study

The satellite soundings used in this statistical structure and correlation function analysis were retrieved from infrared satellite radiances recorded by the Vertical Temperature Profile Radiometer (VTPR) on NOAA 4. Since 1972 the VTPR instrument has been a subsystem on NOAA polar-orbiting satellites which have sun-synchronous orbits with local 0900 and 2100 equator crossing times. Only the morning (local 0900) satellite radiances were used in this study of subsequent severe weather development. Operational temperature retrievals from VTPR radiances are not performed over land areas but only over data-sparse regions, such as the ocean where there are few rawinsonde soundings. However, an iterative method for retrieving temperature profiles over the United States, for example, from full-resolution (~70 km) VTPR radiances, was developed which uses conventional rawinsonde soundings to create an appropriate initial guess profile. The retrieval procedure used in this study is outlined by the authors in a previous article (Hillger and Vonder Harr, 1977).

Rawinsonde soundings create the best initial guess profile when they have close space and time proximity to the satellite radiances. The conventional soundings help determine boundary conditions, such as surface temperature and pressure, which need to be known in any retrieval scheme which uses the radiative transfer equation explicitly. Also the rawinsonde soundings more clearly define the tropospheric lapse rate and moisture content. This information is used to initialize the transmittances or weighting functions for the retrieval process.

The radiance channels and wavelengths for the VTPR instrument as given by McMillin *et al.* (1973) are listed in Table 1. The six 15 μm CO_2 channels, with weighting functions shown in Fig. 1, were used actively in the temperature retrieval algorithm. Spatial changes in these CO_2 channel radiances are a result of

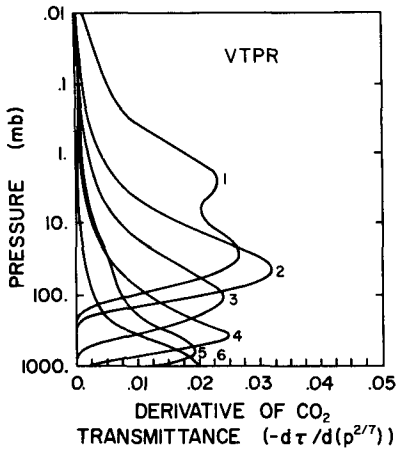

FIG. 1. VTPR CO_2 channel weighting functions for U. S. Standard Atmosphere.

horizontal atmospheric temperature changes in the region of the appropriate channel weighting function. Likewise, the window channel at 12 μm senses primarily surface temperature, but it was not used in the retrieval process. The H_2O channel at $\sim$19 μm was, on the other hand, used passively to obtain moisture information as a residual in the retrieval process. This method of obtaining moisture information from the satellite has been used previously by the authors (Hillger and Vonder Haar, 1977). The moisture information is obtained by a cross correlation between satellite radiance residuals and principitable water values obtained from rawinsondes. Details are available in the cited reference.

The area of interest for this study was centered on National Severe Storm Laboratory (NSSL) mesoscale sounding network shown in Fig. 2. The nine launch

TABLE 2. 1976 NSSL mesoscale rawinsonde network.

Station	ID	Latitude (°N)	Longitude (°W)	Elevation (m)
Clinton Sherman	CSM	35.36	99.20	587
Chickasha	CHK	35.10	97.96	351
Elmore City	EMC	34.65	97.41	320
Fort Sill	FSI	34.67	98.41	360
Hennessey	HEN	36.05	97.89	343
Hinton	HNT	35.47	98.40	510
Altus	LTS	34.66	99.28	419
Seiling	SEL	36.10	98.92	589
Norman	OUN	35.24	97.46	361

sites for soundings taken at both 1500 and 2030 GMT are listed in Table 2. The 1500 GMT (0900 CST) launch time is within 1 h of the NOAA satellite descending (daytime) orbit at approximately 1500–1600 GMT at this latitude. The temperatures and mixing ratios from the NSSL rawinsondes were independently analyzed using statistical structure and correlation functions by Barnes (personal communication) using a method similar to the analysis used for previous years of NSSL data (Barnes and Lilly, 1975). The only active use of the NSSL soundings in this study of satellite soundings was to create an initial guess profile for the iterative retrieval algorithm. All nine soundings at 0900 CST were combined to form one mean profile for each NSSL day. This mean temperature and moisture profile was used as a starting profile in the retrieval of temperatures from the VTPR sounding radiances obtained during the satellite pass on that day.

The subsatellite tracks for the NSSL mesoscale sounding period are shown in Fig. 3. Of the 34 possible days for the NSSL period (10 May–12 June 1976) only 14 days proved to have satellite-sensed radiances which

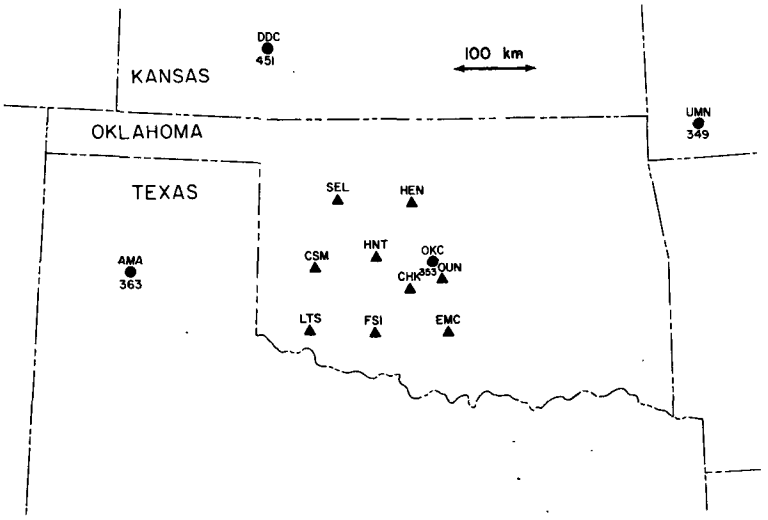

FIG. 2. 1976 NSSL mesoscale rawinsonde network (triangles) and surrounding NWS synoptic rawinsondes (circles)

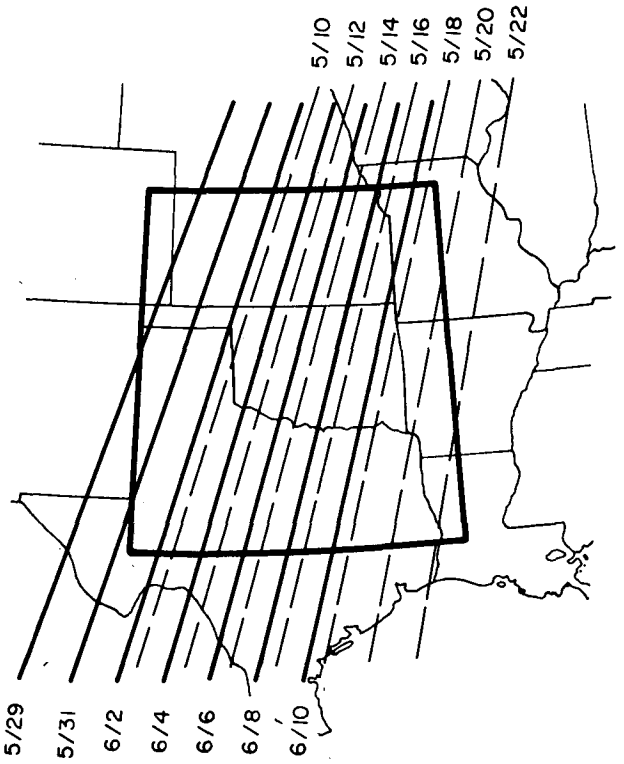

FIG. 3. NOAA 4 descending orbit subsatellite tracks for the 1976 NSSL mesoscale sounding period (10 May–12 June 1976). Each satellite pass provided soundings across most of the designated boundary.

covered most of the selected region around the NSSL sounding grid. The days which were analyzed were every other day between 10 May and 22 May 1976 and between 29 May and 6 June 1976. The polar-orbiting NOAA satellites have an approximate 2-day period for observing the same subsatellite area. The in-between days have subsatellite tracks on either side of the area of interest. The VTPR instrument has a nadir to maximum scan angle distance of ~900 km on the surface of the earth. All possible satellite soundings retrieved within the 9° latitude by 10° longitude box shown in Fig. 3, up to a maximum possible of about 200 soundings per satellite pass, were used for the structure-function and correlation-function analyses of the satellite soundings. This satellite sounding boundary, being about 1000 km on a side, was used to measure the environmental structure around the smaller meso-β scale NSSL network. The box size was chosen to give a large sample on non-cloudy satellite soundings for statistical analysis. Fig. 4 shows the NWS synoptic rawinsonde network within the satellite sounding boundary and surrounding the NSSL rawinsonde network. The NWS rawinsondes were later used in a correlation analysis to verify the information content of the satellite-derived temperature fields for each individual satellite pass.

3. Structure and correlation functions

Statistical structure and correlation functions were used by Gandin (1963) in an objective analysis technique in order to optimally minimize errors of interpolation. Both structure and correlation functions, which are related when normalized, also give a means of comparing data from different instruments which supposedly give the same meteorological measurements. For this reason, both satellite infrared soundings and conventional soundings can be co-analyzed by using these methods. Although results are expected to be dependent on the measuring instrument used and the extent of the analyzed data set, this procedure provides a means for statistical comparison of different measurement systems.

The structure functions as defined by Gandin can be applied directly to pairs of surface or upper air stations. The structure value STR associated with a pair of temperature observation points, for example, is defined as the mean-squared difference between the temperature deviation from the mean at each of the two points $\mathbf{r}_1$ and $\mathbf{r}_2$, i.e.,

$$\mathrm{STR}(\mathbf{r}_1, \mathbf{r}_2) = N^{-1}\sum [T'(\mathbf{r}_1) - T'(\mathbf{r}_2)]^2, \qquad (1)$$

where

$$T'(\mathbf{r}) = T(\mathbf{r}) - \bar{T}(\mathbf{r}) \qquad (2)$$

and $\bar{T}$ is the mean over time for the N observations at each point. This definition is applied to the same pair of temperature observations at N different times.

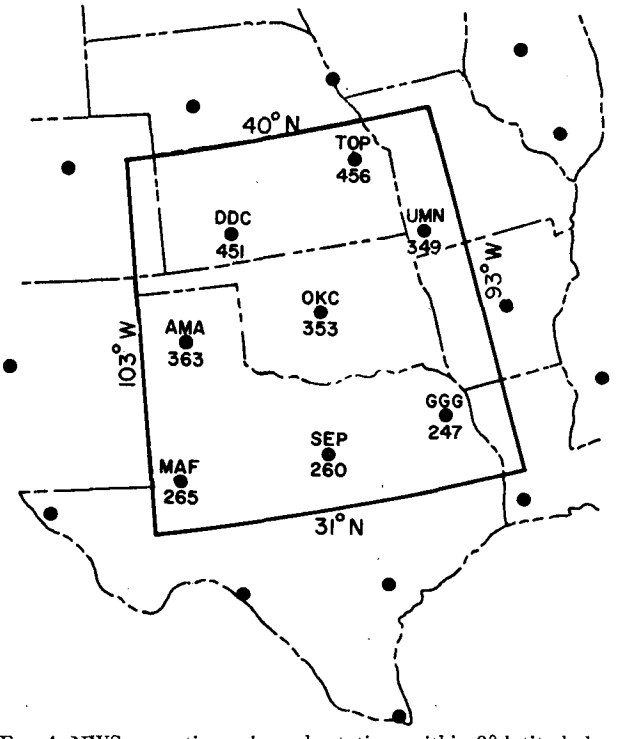

FIG. 4. NWS synoptic rawinsonde stations within 9° latitude by 10° longitude boundary for satellite soundings.

One structure value is then obtained for each possible pair of observations.

To make the assumption that a field is homogeneous with respect to the structure function implies that the structure value depends only on $\mathbf{r}$ which is the vector separation of points $\mathbf{r}_1$ and $\mathbf{r}_2$:

$$\mathbf{r} = \mathbf{r}_2 - \mathbf{r}_1. \tag{3}$$

A homogeneous structure function would be independent of the position of the pair of observations but not independent of their separation distance and direction. To make the further assumption of isotropy as well as homogeneity, the structure function would also be independent of direction and therefore dependent only on the scalar separation distance ρ between $\mathbf{r}_1$ and $\mathbf{r}_2$:

$$\rho = |\mathbf{r}_2 - \mathbf{r}_1|. \tag{4}$$

In this case a line can then be fit to the structure values, one for each pair of observation points. Alternately, the values can be averaged into distance intervals to smooth the structure as a function of pair separation distance.

A closely related function is the covariance function COV whose value for a pair of temperature observations is defined as the mean product of the temperature deviations from the mean at each of the points, $\mathbf{r}_1$ and $\mathbf{r}_2$:

$$\mathrm{COV}(\mathbf{r}_1, \mathbf{r}_2) = N^{-1} \sum T'(\mathbf{r}_1) T'(\mathbf{r}_2). \tag{5}$$

Again, one value is obtained for each possible pair of observations by taking a mean over time. The limiting case of the correlation function occurs when $\mathbf{r}_1 = \mathbf{r}_2$. The covariance then equals the temperature variance at the point $\mathbf{r}$, i.e.,

$$\mathrm{VAR}(\mathbf{r}, \mathbf{r}) = N^{-1} \sum [T'(\mathbf{r})]^2. \tag{6}$$

The relationship between the structure and correlation function can be shown to be

$$\mathrm{STR}(\mathbf{r}_1, \mathbf{r}_2) = \mathrm{VAR}(\mathbf{r}_1, \mathbf{r}_1) + \mathrm{VAR}(\mathbf{r}_2, \mathbf{r}_2) - 2\,\mathrm{COV}(\mathbf{r}_1, \mathbf{r}_2), \tag{7}$$

where the first two terms are the variances of the temperature deviations at observation points $\mathbf{r}_1$ and $\mathbf{r}_2$, respectively, and the third term is the covariance between temperature deviations at points $\mathbf{r}_1$ and $\mathbf{r}_2$. With the assumptions of homogeneity and isotropy the structure function becomes

$$\mathrm{STR}(\rho) = 2\,\mathrm{VAR}(0) - \mathrm{COV}(\rho) \tag{8}$$

since the variance is assumed homogeneous. In the limiting case of zero separation distance $\mathrm{STR}(0) = 0$ when there is no noise in the data, and at large separation distances $\mathrm{STR}(\infty) = 2\,\mathrm{VAR}(0)$, because generally the covariance will decrease to zero.

The correlation function CORR, which will be used here instead of the covariance, arises by normalizing the covariance function by the variance:

$$\mathrm{CORR}(\rho) = \frac{\mathrm{COV}(\rho)}{\mathrm{VAR}(0)}. \tag{9}$$

Again, there is only one variance value because of the homogeneity assumption.

Both the structure and correlation functions will be utilized to compare satellite-derived temperatures and moisture with high-density conventional soundings without comparing the temperatures directly. Changes in the structure function with distance are equivalent to mean gradients in the observed fields. For the assumptions of homogeneity and isotropy, which will be used throughout this study, the structure and correlation functions are nondirectional, and they apply to any position in the analyzed fields of data.

When applying the structure and correlation functions to the satellite data, there are no unique pairs of observations points which produce a structure or correlation value by taking a mean over time. The satellite radiometer does not sense exactly the same points in different satellite passes. Therefore the definitions of structure and correlation functions have to be modified for this different type of data. Instead of unique pairs of observation points, one structure value is calculated for all possible pairs of points with a separation distance between certain limiting values. This allows only one structure or correlation value within each distance interval, instead of several values for different pairs of observation points which have similar separation distances.

The structure-function definition for satellite-derived temperature observations in the homogeneous and isotropic case becomes

$$\mathrm{STR}(\rho_k) = \sum_{i,j:\, j>i}^{\rho_k<\rho<\rho_{k+1}} [T(\mathbf{r}_i) - T(\mathbf{r}_j)]^2 \Big/ \sum_{i,j:\, j>i}^{\rho_k<\rho<\rho_{k+1}} 1, \tag{10}$$

where the summation is taken over all possible pairs of satellite observations regardless of their orientation. One structure value is obtained for each 50 km interval from 50 to 1000 km (i.e., 50–100 km, 100–150 km, etc). The structure value for each interval includes all pairs of temperature observations whose separation distance is within the specified limits, and the number of values within each interval (the denominator) is equal to number of pairs within that interval. The condition that $j > i$ avoids including each pair twice or including coincident points. If the satellite observations are numbered $i = 1, 2, \ldots, M$, then the total number of combinations within all distance intervals is $M(M - 1)$. Notice also that the observations are temperatures and not temperature deviations. Both would give the same result, since the mean value to be subtracted from each temperature would be the same. The mean and variance calculated over i or j would include the same elements and would therefore be the same.

Similarly the correlation function for satellite-derived temperature observations is modified to become

$$\mathrm{CORR}(\rho_k) = \sum_{i,j:\,j>i}^{\rho_k<\rho<\rho_{k+1}} T'(\mathbf{r}_i)T'(\mathbf{r}_j) \Big/ \sum_{i,j:\,j>i}^{\rho_k<\rho<\rho_{k+1}} [T'(\mathbf{r}_i)]^2. \quad (11)$$

In this case the observations are temperature deviations from a spatial temperature mean over the summation within each separation interval. The numerator is the covariance and the denominator the variance of the paired values. Again the total number of pairs in all intervals is $M(M-1)$ for M observations, and the summation is taken over all possible pairs of points regardless of orientation.

With these definitions, it is possible to calculate structure and correlation values within each distance interval for a single field of satellite observations. In order to compare the results with the structure and correlation function analyses from the NSSL high-density rawinsondes, the summations were also taken over all 14 days of satellite observations during the NSSL sounding period. Later individual fields of satellite observations were analyzed to note variations in the structure functions on a day-by-day basis.

To see how random noise in the satellite observations affects the structure and correlation functions, we simply add a noise element (uncertainty) to the temperature values, i.e.,

$$T^*(\mathbf{r}) = T(\mathbf{r}) + \delta(\mathbf{r}), \quad (12)$$

where δ is the uncertainty in T^* and T is the actual temperature value. For the homogeneous and isotropic assumptions the covariance function is unaffected by random noise for all but the case when $\mathbf{r}_1 = \mathbf{r}_2$. This is because the noise in each of a pair of observations is uncorrelated. In other words, only for coincident values does the variance increase by a value equal to the noise variance

$$\mathrm{VAR}^*(0) = \mathrm{VAR}(0) + \sigma^2, \quad (13)$$

where

$$\sigma^2 = \overline{\delta^2} \quad (14)$$

is the mean squared uncertainty for homogeneous noise (independent of r).

The correlation function is then decreased by the factor $\mathrm{VAR}(0)/[\mathrm{VAR}(0) + \sigma^2]$ so that it becomes

$$\mathrm{CORR}^*(\rho) = \frac{\mathrm{CORR}(\rho)}{1+\sigma^2/\mathrm{VAR}(0)}. \quad (15)$$

Now the structure function, being the sum of twice the variance minus the covariance at any separation distance, becomes

$$\mathrm{STR}^*(\rho) = \mathrm{STR}(\rho) + 2\sigma^2. \quad (16)$$

In this case, the noise-included structure function is increased in value by twice the mean-squared error. The structure value at zero separation distance will then become

$$\mathrm{STR}^*(0) = 2\sigma^2 \quad (17)$$

instead of a no-noise value of zero. This makes it easy to determine the noise level or uncertainty in the observed values by extrapolating the structure to its value at zero separation. The extrapolation was accomplished assuming that the structure function is linear at small distances. Two estimates of the uncertainty using different points to fit the linear extrapolation were made. A mean noise value was used as the estimated noise level. Applying this value to the correlation function, the correlation results were then corrected for this uncertainty to allow the correlation to attain a value of 1.0 at zero separation distance.

The method of elimination of the random noise, by extrapolating the structure function to zero separation distance ($\rho = 0$), gives a value equal to twice the mean-squared noise $2\sigma^2$ in the observations. This value is only a measure of random noise in the satellite-derived products. No bias or systematic errors were included. However, this uncertainty σ is also an estimate of the minimum spatial resolution necessary for measuring these atmospheric variables from satellites. Natural atmospheric variability of lesser magnitude than the estimated noise level will not be measured, and measurements are unnecessary at higher resolution than the separation distance at which the structure function attains this minimum noise value.

4. Analysis of VTPR radiances

A structure and correlation analysis of the VTPR radiances was performed along with the analysis of the temperatures and moisture derived from the radiances. Gradients in the VTPR radiances, which relate to temperature or thickness gradients, could then be detected directly. If the structure functions of the radiances contain the same gradient information as those of the satellite-derived temperatures, then it may not be necessary to revert to the temperature retrieval process. A decision on whether or not to retrieve temperature profiles from the radiances could be made depending on the radiance structure. The determination of small-scale gradients from satellite data could also signal the need for other types of measurements. Otherwise, high-resolution measurements may not be necessary when such temperature and moisture gradients are not present.

The structure function and correlation analyses were performed on all of the VTPR calibrated radiance channels, but only radiances from relatively clear columns were used. All columns with a window channel (channel 8) radiance below 100 mW/(m^2 sr cm^{-1}) were not used in the analysis to avoid severe cloud contamination problems, but this did not eliminate

cloud problems entirely. Columns with small amounts of cloud in their field of view may still have radiances above this threshold. The VTPR CO_2 channels 1–6 sense temperatures in layers at progressively lower levels in the atmosphere. The H_2O channel has a weighting function maximum which is highly variable depending on the magnitude and vertical distribution of the moisture profile used to initialize the transmittance functions. All weighting functions are rather broad, so the radiances represent an integration of temperature and moisture effects over a rather large vertical depth. The CO_2 channels are mainly sensitive to temperature, but the CO_2 channels which sense lowest in the atmosphere are also affected by clouds and the variable moisture content in the lower troposphere.

The results of the structure-function analysis for the temperature-sensing CO_2 channels 4, 5 and 6 are shown in Fig. 5. One structure value was plotted for each 50 km wide separation interval starting at 50 km. Because the maximum resolution of the VTPR instrument is about 60–70 km, the first category extends from 50 to 100 km, and the obtained structure value was plotted at 75 km. The maximum separation distance at about 1000 km was chosen because of the size of $9° \times 10°$ box. Relatively few pairs of soundings extended up to the 1400 km diagonal length of the box.

Two lines are plotted for each channel in Fig. 5. The solid lines are the structure functions for all radiance columns with channel 8 radiance greater than the chosen 100 mW/(m² sr cm⁻¹) noncloud threshold. These lines would represent the true structure of the VTPR radiances except for an additional variation in radiance as a function of zenith angle. As the satellite radiometer scans from side to side the weighting functions for each channel change as the zenith angle of the satellite scan changes with respect to the surface of the earth. The zenith angle is the angle between the satellite-sensed column and a vector normal to the surface of the earth. An adequate correction to the radiances in terms of $\sec^{\frac{1}{2}}\theta$, where θ is the zenith angle, was noted by Duncan (1977) and Grody and Pellegrino (1977). This correction was calculated for a small sample of temperature profiles and is equivalent to the correction made by the retrieval algorithm for non-nadir scan positions. The radiance change from that of a zenith angle of zero is an increasing function of θ. For CO_2 channels which sense low in the atmosphere the radiance change is negative (limb darkening), but for CO_2 channels 1 and 2 the radiance change is positive (limb brightening) because these channels sense temperatures above the tropopause. These changes are not linear. However, when plotted as a function of $\sec^{\frac{1}{2}}\theta$ these changes are linear to within the uncertainty of the radiances.

Since the correction for each radiance channel is linear in terms of $\sec^{\frac{1}{2}}\theta$, it is easy to determine the magnitude of the correction at any zenith angle and to apply that correction to the observed radiances. The

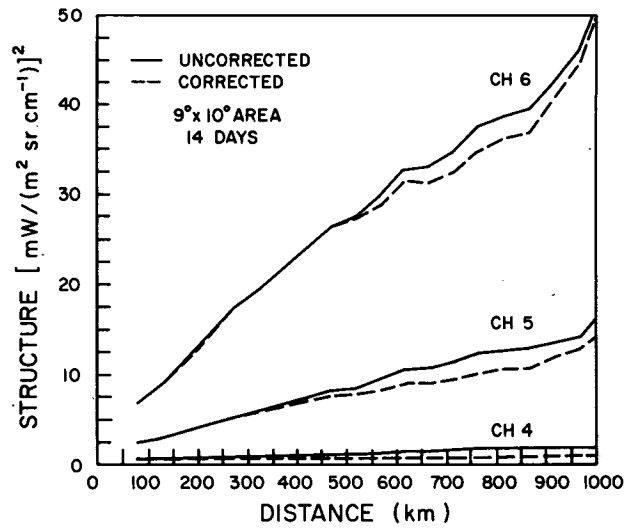

FIG. 5. Structure as a function of satellite sounding separation distance for scan-angle corrected and uncorrected radiances for VTPR CO_2 channels 4, 5 and 6.

maximum correction was approximately 4 mW/(m² sr cm⁻¹) for channels 5 and 6 at a zenith angle of 38°. The corrected radiances were then analyzed to obtain the dashed (corrected) structure functions in Fig. 5. The main effect of these corrections was to increase the covariance (decrease the structure function) at large separation distances. As should be expected, the correction should cause a minimum relative change between adjacent scan positions and a maximum relative change between nadir and maximum scan positions. For the VTPR instrument the distance between the nadir (subsatellite) position and the maximum zenith angle of 38° on either side of the subsatellite track is roughly 900 km. The difference between the uncorrected and corrected structure functions does also appear to reach a maximum at approximately this same distance.

The number of pairs of radiances in each distance interval for both the uncorrected and corrected cases are shown in Fig. 6. The radiance pairs for all 14 days were combined in the structure analysis, so as to include several different synoptic situations. The relative changes of 1000 or more pairs for intervals between 200 and 700 km is due to an interaction between the variable spacing of the VTPR sounding positions and the fixed 50 km analysis intervals. Only at large separation distances is the number of pairs small enough so the results of the structure analysis may be questioned because of sample size. If the data sample is halved the structure function remains virtually the same except at the largest separation distances. According to Gandin, a test for a sufficiently large data set is when the structure function is rather smooth and its magnitude is not affected by the amount of data in the analysis.

The major point to be noted about the structure functions in Fig. 5 is that they represent mean non-

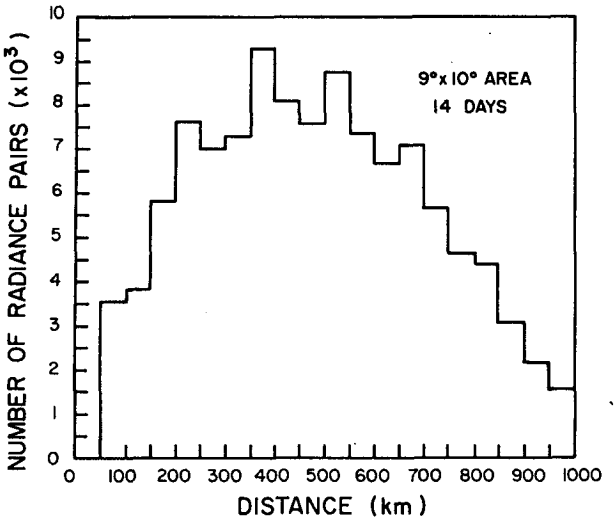

FIG. 6. Number of radiance pairs in each 50 km separation interval for radiances >100 mW/(m² sr cm⁻¹).

directional gradients in the observed fields over the 14 days examined. The structure function for channel 4 is fairly linear and shows little change in slope with distance, but the structure functions for channels 5 and 6 show a tendency to increase more rapidly at smaller separation distances than at larger distances. This greater slope at smaller distances (note especially the lines for corrected radiances) is an indication of higher frequency or shorter wavelength components in the observed fields for the CO_2 channels with weighting function maxima lowest in the atmosphere. (The structure function for a pure sine wave pattern would actually return to zero at some finite distance after attaining its maximum value.) These higher frequency components can be caused by small-scale temperature and water vapor changes in the lower troposphere.

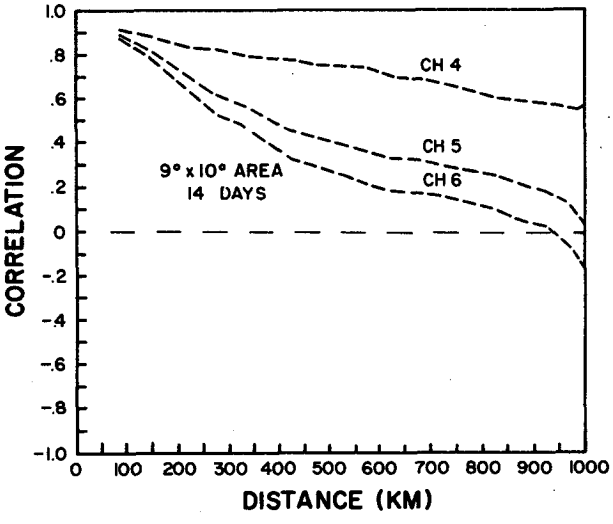

FIG. 7. Correlation as a function of satellite sounding separation distance for scan-angle corrected radiances for VTPR CO_2 channels 4, 5 and 6.

However, cloud contamination could also cause small-scale variability in the radiances for channels 5 and 6. The structure function for channel 4 shows much less variability due to moisture and cloud contamination because of its higher tropospheric weighting function maximum. Note also the progressive increase in the structure values for channels 4, 5 and 6. Much larger structure function values are obtained at all distances for the more highly variable lower tropospheric temperatures.

When the correlation functions for VTPR radiance channels 4, 5 and 6 are plotted on the same graph in Fig. 7 the differences can be seen more easily. The correlation functions eliminate the absolute magnitude changes between the individual structure functions. The lowest tropospheric channels again show greater slope at small separation distances and less correlation (more structure) at all distances. The correlation function for channel 6 has the smallest values and decreases to zero correlation at ~900 km. In the mean only within a distance of up to 900 km from a single point are the adjacent values positively correlated. So this separation distance would be far beyond the maximum separation to allow meaningful interpolation of the satellite soundings. Since it is desirable to have a reasonably large correlation between adjacent sounding positions in order to attempt any interpolation, a much smaller spacing of soundings is necessary. The slope of the correlation function is also used to determine the weights assigned to data points in optimum interpolation. Less weight should be given to outlying points in an area of little correlation than in an area of high correlation.

The radiance structure functions in Fig. 5 also give us the noise level or uncertainty in the radiances. All structure functions were extrapolated to zero distance to obtain a value equal to twice the mean squared random error $2\sigma^2$ in each channel [see Eq. (17)]. The rms extrapolated errors are listed in Table 3 along with the mean and standard deviation of all radiances for each channel. The maximum rms error values in

TABLE 3. Radiance errors. All units mW/(m² sr cm⁻¹).

Channel	Radiance Mean	Radiance Standard derivation	rms error Maximum	rms error Extrapolated	Sensitivity*
1	60.0	0.82	0.48	0.47	0.75
2	47.7	0.76	0.23	0.21	0.25
3	44.4	0.60	0.23	0.21	0.25
4	56.4	0.92	0.39	0.33	0.25
5	77.5	2.38	1.04	0.77	0.25
6	95.3	4.09	1.82	1.26	0.25
7 (H_2O)	116.1	5.26	1.95	0.87	0.25
8 (window)	120.1	8.53	3.88	2.66	0.25

* Maximum allowable relative error (McMillin *et al.*, 1973).

Table 3 were obtained by assuming that the structure functions obtain their smallest values (become flat) at the smallest separation interval of 75 km which includes all pairs of adjacent scan spots. The maximum and extrapolated rms errors are similar for all but CO_2 channels 5 and 6 which have low tropospheric maxima and for the H_2O and window channels. These channels have significant structure at small separation distance, which implies that they are sensing small-scale features in the observed fields even at the maximum resolution of the VTPR instrument. Some of this small-scale structure may be due to cloud contamination which remains in the radiances. Another indication of small-scale variability is seen by comparing the rms extrapolated errors to the sensitivity values in the last column of Table 3. These sensitivities are maximum allowable relative error values obtained before the launch of the VTPR instrument. The values for the upper tropospheric and stratospheric channels compare favorably to the extrapolated rms noise levels, but the lower tropospheric channels have exaggerated rms noise levels due to small-scale variability remaining in the radiances.

5. Analysis of satellite-derived temperatures and moisture

The structure and correlation function analysis was applied in a similar manner to the temperature and moisture derived from the radiances. Temperatures at three levels, 300, 500 and 700 mb, were chosen for analysis, as well as the radiance residual for the H_2O channel (channel 7). The H_2O residual has been shown to be proportional to the precipitable water in the observed column (Hillger and Vonder Haar, 1977). The residual at any point is defined as the difference between the observed and calculated (observed minus calculated) radiance for the H_2O channel. The calculated radiances are computed from the derived temperature profile, and if the derived temperature profile is reasonably close to the actual temperature profile, then the main difference between the observed and calculated H_2O radiances should be due to moisture effects. Moisture differences usually exist between the initial guess and actual profiles.

Weinreb (1977) has shown that these errors in prior estimates of water vapor propagate into the solution for the temperature profile in the retrieval process. This error is largest in the case when one initial guess profile is used across large moisture gradients. Briefly, the effect on the derived lower tropospheric temperatures is as follows: If the initial guess moisture amount is too small, then the calculated CO_2 channel radiances are exaggerated. The iterative process is designed to compensate for calculated radiances which are too high compared to observed radiances by decreasing the retrieved temperatures in the lower troposphere. These low retrieved temperature values are then due to the underestimated initial guess moisture profile.

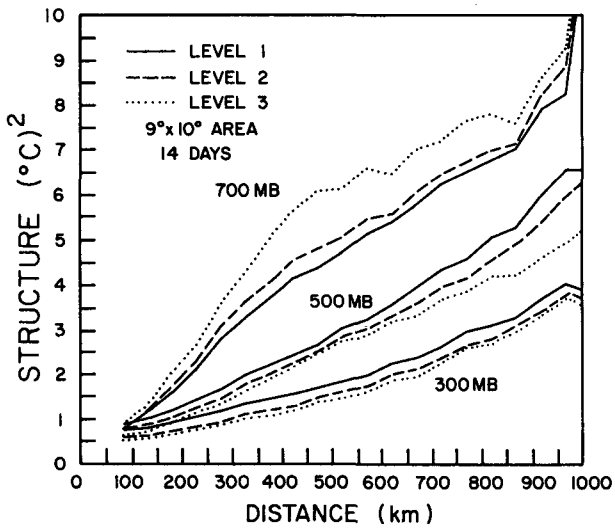

FIG. 8. Structure as a function of sounding separation distance for satellite-derived temperatures at 300, 500 and 700 mb for three noncloud thresholds.

The same reasoning applies to an initial guess profile which is too moist. In that case, the lower tropospheric temperatures are overestimated. Therefore, these error sources show the need for an active role of the moisture channel in the temperature retrieval process, rather than the passive role used here. Some active feedback mechanism needs to be introduced to better utilize the moisture information in the VTPR H_2O channel. Further research is continuing in this area.

The structure function for the satellite-derived temperatures and moisture are shown in Figs. 8 and 9. Again, data for all 14 days were combined into the structure analysis. The results were categorized into 50 km wide intervals as were the structure functions of the radiances shown previously. Three lines occur on

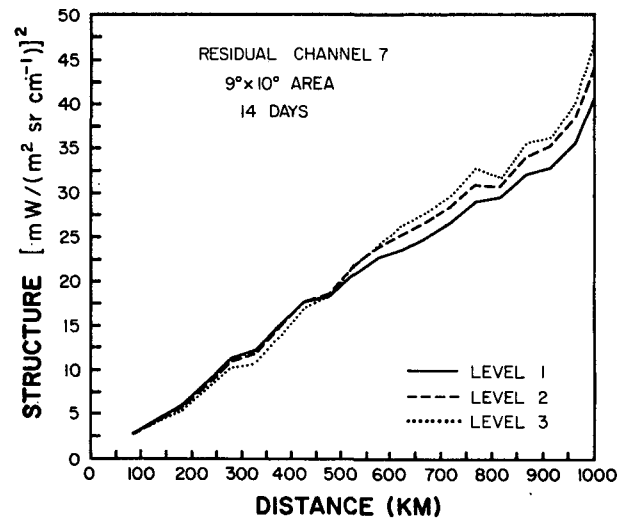

FIG. 9. As in Fig. 8 except for satellite-derived moisture (residual H_2O channel 7) for three noncloud thresholds.

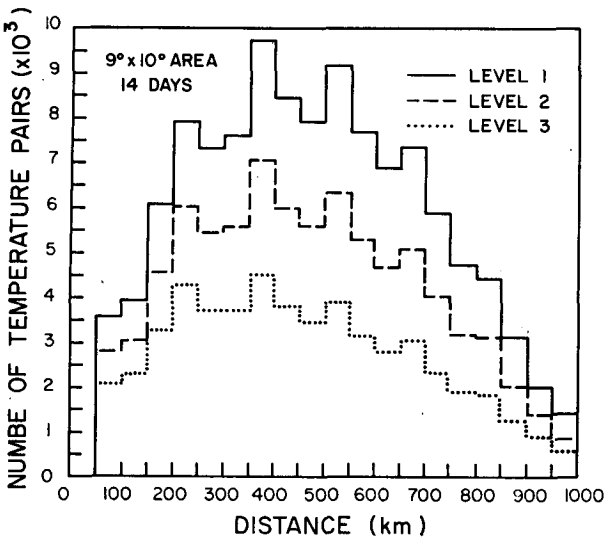

FIG. 10. Number of satellite-derived temperature pairs in each 50 km separation interval for three noncloud thresholds.

each graph. The difference between the lines is due to different cloudiness thresholds. The temperature retrieval alogorithm incorporates a very simple one-parameter cloud correction technique (Shaw *et al.*, 1970). The idea is to compensate where possible for the most severe cloud contamination. To do this, radiances calculated for the initial guess profile are compared to observed radiances at each spot.

The major difference between the initial guess and actual temperature profile at this point is assumed to be due to the effects of clouds. The observed radiances for the CO_2 channels with low tropospheric maxima will be affected the most. The observed radiances will be low because of an elevated cloud level above the earth's surface. To estimate this cloud level, the integration of the calculated radiances is performed assuming that the cloud cover is 100% and that it occurs at progressively higher levels. The residuals between the observed and calculated radiances for CO_2 channels 4, 5 and 6 are used as the predictor. A minimum in these residuals will occur when an equivalent cloud pressure is obtained by progressively starting the integration at higher levels. No cloud amount information is available since the obtained level is assumed to be completely cloud covered.

Three thresholds were chosen to designate the separation between cloud and noncloudy sounding columns. For each variable in Figs. 8 and 9, three structure functions were calculated based on noncloudy soundings according to the chosen cutoff pressures of 700 mb (level 1), 800 mb (level 2) and 900 mb (level 3). The least stringent cloud, no-cloud cutoff at 700 mb allowed soundings to be included in the structure calculation even if clouds were estimated to be below 700 mb. Similarly for 800 mb, but for 900 mb the cloud, no-cloud threshold is so low (the surface pressure is about 950 mb in this region) that virtually no soundings with any detected clouds were included in the calculations. These structure functions were the most cloud-free and were possibly the closest to the true clear-air structure values. The other structure functions illustrate the effects of clouds on the calculated structure and noise estimates.

The structure functions for temperatures at 300 and 500 mb in Fig. 8 tend to have greater slope at larger separation distances. The fact that the structure functions tend to become flat, especially for 300 mb temperatures, around the 100 km distance means that there appears to be little observed small-scale structure (gradient) in the temperatures near this minimum separation distance. The structure value has approached a minimum value which is an estimate of the uncertainty in the retrieved temperatures. These structure functions, however, are an indication of the mean nondirectional gradient for all 14 days and not of the larger or smaller gradients which may occur in some particular synoptic situations.

The structure functions for 700 mb temperatures in Fig. 8 and the moisture residuals in Fig. 9 have their maximum slope at smaller separation distances. This is an indication of higher frequency components in the 700 mb temperature and moisture fields than in the 300 and 500 mb temperature fields. Both structure functions maintain large slopes at the minimum separation distance of 75 km which indicates a need for measurements of lower tropospheric temperatures and moisture at the resolution of the VTPR instrument. Even though these structure functions may have reached their minimum values at this minimum separation distance, there will remain some days when the observed gradients in temperature or moisture are different than these statistical mean gradients.

Increasing the cloud, no-cloud cutoff pressure level decreased the number of usable temperature pairs as shown in Fig. 10. A change from levels 1 to 3 reduced the number of temperature pairs to almost half. The more stringent cloud thresholds (levels 2 and 3) also decreased the structure and estimated noise values for temperatures at 300 and 500 mb in Fig. 8. These structure functions decreased because of reducing the variability in the measurements by eliminating possibly cloudy values. However, the structure function for 700 mb temperatures did increase with low-cloud cutoffs. This may be explained by the remaining uncertainty in 700 mb temperatures due to variable moisture in the lower troposphere. Radiances from cloudy columns contain little lower tropospheric moisture informations whereas clear columns contain the most moisture information since most moisture resides in the lowest tropospheric levels. Any unexplained moisture gradients would then increase the variability of the 700 mb temperatures to a larger extent than the other temperature levels examined. The 700 mb level is near the weighting functions maximum for the VTPR H_2O channel.

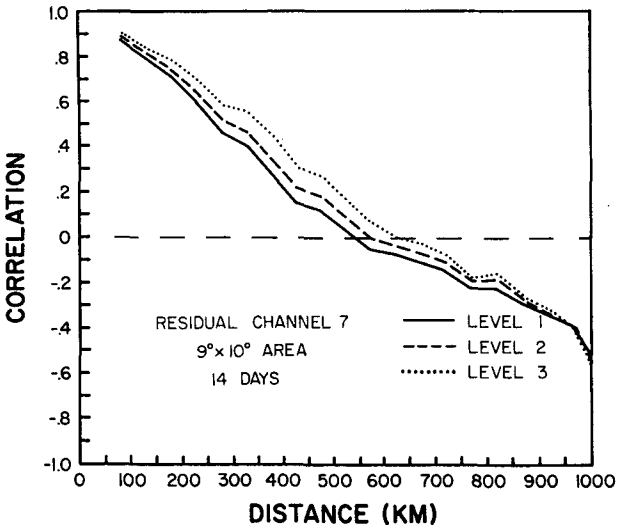

FIG. 11. Correlation as a function of sounding separation distance for satellite-derived moisture (residual H_2O channel 7) for three noncloud thresholds.

The correlation function for the H_2O residual is shown in Fig. 11. For the level 3 cloud threshold, the correlation function approaches zero correlation at about 600 km. Again, as for the radiances for channel 6 which contain temperature and moisture information, this zero correlation implies that in the mean no moisture information can be implied beyond 600 km from a single measurement. Measurement resolution much better than 600 km needs to be attained in order to be assured of high enough correlations to be able to interpolate between moisture measurements from this satellite information. Because of the rapid decrease in correlation at small separation distances, the need for high-resolution information is imperative, especially on days with larger moisture gradients. If this mean correlation function representation is a correct one for moisture, then any moisture analysis created from rawinsonde data cannot be successfully interpolated beyond a distance of 300 or 400 km from a single rawinsonde launch site. Much stronger gradients, however, would require more closely spaced soundings.

As was accomplished for the VTPR calibrated radiances, all structure functions were extrapolated to zero separation distance to obtain rms noise levels for retrieved temperatures. This was done for the cloud, no-cloud threshold at 900 mb (level 3), although results were only slightly higher for other levels. Extrapolated and maximum noise levels are shown in Table 4 along with mean and standard deviation for each value. The mean noise level of $\sim$0.5°C for temperatures at 300, 500 and 700 mb is not unreasonable for satellite-derived temperatures. The reason this value is much smaller than the standard error of 1–3°C usually associated with satellite-rawinsonde comparisons is due to the fact that this value is the rms noise level for satellite-derived temperatures only. It is not a measure of any bias which may exist between the satellite and rawinsonde temperatures. These numbers then indicate the maximum temperature resolving capability of the VTPR sounding instrument for temperatures derived by the retrieval method used here.

The estimated uncertainties for 300 and 500 mb temperatures at the minimum and zero separation distance are very similar, but the larger difference between the maximum and extrapolated rms noise levels for the moisture residuals does indicate the small-scale or high spatial variability of moisture. The moisture noise level cannot be reliably extrapolated below the approximate 1.1 mW/(m^2 sr cm^{-1}) maximum rms error value because the structure function may exhibit significant change in slope at small distances. To better understand the magnitude of this radiance residual noise level, an equivalent total precipitable water and its associated noise level are also given. These values were calculated from the equation for the linear regression line between radiance residuals and precipitable water found by the authors (Hillger and Vonder Haar, 1977) for 24 April 1975. This uncertainty value, calculated by the regression equation in Table 4, of 0.22 cm of water is about 11% of the total precipitable water and only represents an order of magnitude noise level obtainable by this method. The actual precipitable water and noise level for any case study day depends on the relationship between radiance residuals and precipitable water for that day. No regression lines were computed for the case study days examined here because of the small number of coincident points and the small magnitude of moisture gradient found on many days in the mesoscale rawinsonde soundings.

6. Comparisons to NSSL mesoscale structure and correlation functions

The structure and correlation functions for the satellite-derived temperatures and moisture were compared to structure and correlation functions for temperature and moisture information from the 1976 NSSL mesoscale soundings. The NSSL soundings were

TABLE 4. Temperature and moisture errors.

Value	Mean	Standard deviation	rms error: Maximum	rms error: Extrapolated
300 mb T (°C)	−40.6	2.30	0.47	0.42
500 mb T (°C)	−13.5	2.59	0.53	0.46
700 mb T (°C)	5.5	3.67	0.64	0.25
H_2O radiance residual* [mW/(m^2 sr cm^{-1})]	−1.73	3.68	1.09	0.35
Precipitable water** (cm)	1.95	0.74	0.22	0.07

* Residual $= N_{observed} - N_{calculated}$ (H_2O channel).

** Assuming PW (cm) $= 1.6 - 0.2 \times H_2O$ radiance residual (Hillger and Vonder Haar, 1977).

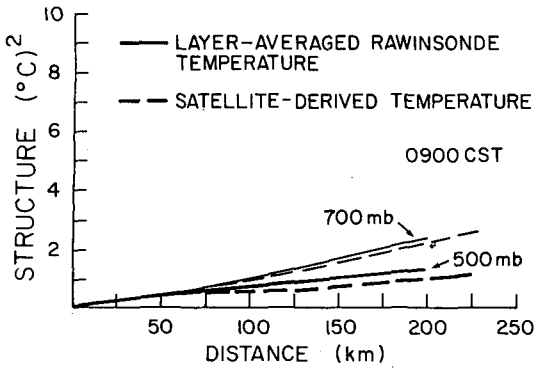

FIG. 12. Comparison of temperature structure values at 500 and 700 mb for satellite retrievals with similar structure values (from Barnes, 1977) for NSSL rawinsondes.

launched at 1500 GMT (0900 CST), within 1 h of the satellite soundings at 1500–1600 GMT. The analysis of all 34 days of NSSL soundings was performed by Barnes (personal communication) in a manner similar to that used on NSSL data from 1966–68 (Barnes and Lilly, 1975). The 34-day composite results for NSSL layer-averaged rawinsonde temperatures at 500 and 700 mb are shown as solid lines in Fig. 12. The structure functions were fit to data points, one point corresponding to all soundings at 1500 GMT for a given pair of stations in the NSSL network shown in Fig. 2. For the nine NSSL launch sites there are 36 possible pairs of stations ranging from about 50–200 km apart. The structure functions were also forced to a value of zero at zero separations distance, so no equivalent noise level was estimated for the NSSL rawinsonde data.

The dashed lines in Fig. 12 are portions of the corresponding structure functions for satellite-derived temperatures at 500 and 700 mb. These satellite-derived structure values are the ones for the least cloudy, level 3 threshold. At the smallest separation distance of 75 km for the satellite data, the solid and dashed lines intersect showing an equivalent relative uncertainty for the two systems at this separation distance. However, at larger distances, the structure-function values for the satellite-derived temperatures are less than those for the rawinsonde temperatures. The 500 mb structure functions differ by a maximum of about 0.4°C² at 200 km which corresponds to a systematic temperature gradient difference of 0.6°C over 200 km. This small difference could be easily explained by the different vertical depths over which the temperatures were averaged. Barnes used a 900 m vertical averaging depth, while the satellite temperatures are inherently averaged over a larger vertical depth. The larger vertical averaging depth for the satellite data would cause less variability or less structure between pairs of measurements.

Several papers have dealt with the vertical resolution of satellite soundings including those of Conrath (1972) and Rodgers (1976). All vertical resolution studies deal with the tradeoff between vertical resolution and noise. Conrath determined an intrinsic vertical resolution of 300 mb (or 4500 m) at the 500 mb level. The resolution does increase with atmospheric pressure and decrease with height. However, Thompson *et al.* (1976) showed that anomalies with characteristic thickness less than this theoretical resolving length can be sensed by VTPR. Since the vertical resolution is much poorer in the case of satellite-derived temperatures, this may be the main reason for decreased structure even though the statistical samples in each case were overlapping in time but not necessarily equivalent.

Fig. 13 shows the correlation functions for moisture. Correlation functions were used to eliminate problems with differences in units between moisture structure functions. The solid and dot-dashed lines are results for 900 m layer-averaged rawinsonde mixing ratios at 700 and 500 mb, respectively. The dashed line is the correlation function for the satellite moisture residuals. The much higher correlations at larger distances for the satellite data are due to the vertical integrating or smoothing effect of the one moisture value derived from the satellite radiances. This integration reduces the effect of higher order changes which can occur at one or several atmospheric levels. The correlations for the layer-averaged mixing ratios at 700 mb are also higher than those for 500 mb. Most atmospheric moisture resides in low tropospheric levels with only occasional mixing to higher levels.

The structure functions for temperatures compared favorably for the two data sets, considering the inherent vertical-averaging differences, but the moisture correlation functions did not approach this similarity. The much lower correlations for the rawinsonde mixing ratios show that stronger gradients than sensed by the satellite-derived radiance residuals are present at 500 and 700 mb even in the mean. Therefore, the integrated moisture information from satellite measurements does not equal the information content in terms of gradients which can be obtained from mesoscale rawinsonde soundings. The main difference is due to the

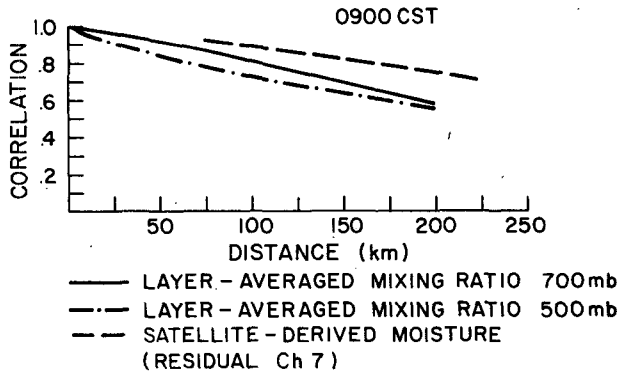

FIG. 13. Comparison of moisture correlation values for satellite measurements with layer-averaged rawinsonde mixing ratio correlation values (from Barnes, 1977) at 500 and 700 mb.

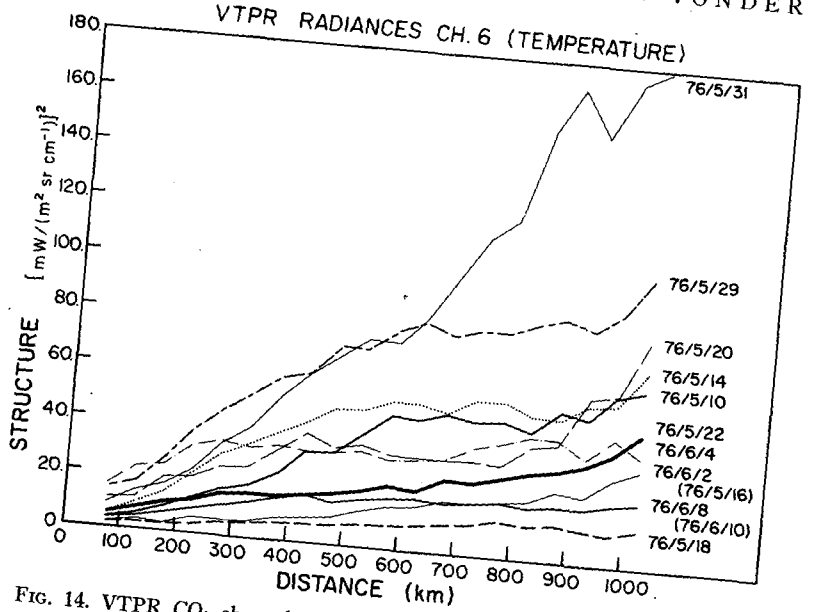

FIG. 14. VTPR CO_2 channel 6 radiance structure at a function of sounding separation distance for individual satellite passes at approximately 0900 CST on each day.

lack of vertical moisture information in one satellite moisture value.

7. Structure functions for individual days

The structure-function analysis was applied on an individual basis to each satellite pass at approximately 1600 GMT. It must be remembered that the assumptions of homogeneity and isotropy are less valid for one day of data than for the combined data set. Another problem with this approach is that some days may be too cloudy and may not contain a large enough sample of cloud-free radiances for statistical analysis. However, if there are enough cloud-free columns, then the structure function will detect a mean nondirectional gradient for that day. This mean gradient of temperature or moisture can help determine if there is a possiblility of severe weather events later that day. Large or sharp gradients in temperature and moisture usually are necessary for the development of lines of summertime convective activity and subsequent severe weather. These gradients can be determined from high-resolution conventional soundings, but the satellite radiances are also capable of detecting these gradients without any conventional sounding information.

The structure functions for the scan-angle-corrected radiances for channel 6, the lowest tropospheric CO_2 channel, for 10 of the 14 case study days are plotted in Fig. 14. Two days were too cloudy to contain a large enough statistical sample, and two other days were not plotted to avoid overcrowding the figure. The structure functions for these two days were similar to other days already plotted. The radiance values analyzed were for clear sounding columns with a window channel radiance above the 100 mW/(m² sr cm⁻¹) threshold.

Table 5 lists the significant weather events and times, if any, for all 14 days on which the structure-function analysis was applied. These weather events were gathered from severe weather reports in Oklahoma and northern Texas, the area for which the radiances were obtained. Five of the days had no significant weather activity. The remaining days either reported thunderstorms or hail. Two days in particular, 29

TABLE 5. Significant surface weather events for NSSL days.

Date	Cloud cover* at about 1600 GMT	Significant weather	
		Event	Time**
(1976)			(GMT)
10 May	2	hail	0600–0700
12 May	4 (cloudy)	hail	1715–0040
14 May	2	no activity	
16 May	3	no activity	
18 May	1 (clear)	no activity	
20 May	3	thunderstorms	
22 May	3	hail	0105–0335
29 May	2	funnel clouds —hail	2300–0300
31 May	3	funnel clouds —hail	2200–0200
2 June	1 (clear)	thunderstorms†	
4 June	2	thunderstorms†	
6 June	4 (cloudy)	thunderstorms†	
8 June	2	no activity	
10 June	2	no activity	

* Approximate cloud cover from window channel radiances on a scale of 1 to 4. (1 = mostly clear, 4 = mostly cloudy).

** From *Storm Data* reports (May–June 1976) (Oklahoma and North Texas).

† From 2345 GMT SMS visible images or NOAA SR images.

and 31 May 1976, had reports of both funnel clouds and hail. These two days also had the largest structure-function values shown in Fig. 14 at separation distances of as little as 200 km. Since the VTPR channel 6 radiance is affected mainly by the temperature in the lower troposphere, the slopes of these structure values reflect the magnitude of lower tropospheric temperature gradients. On the other hand, the days with no significant weather activity showed the smallest structure values. For example, 18 May 1976, which was clear, had the lowest structure values at almost all separation distances. On this day, there was little increase in the observed temperature structure with distance as sensed by the radiance for VTPR channel 6.

Table 5 also gives an indication of the cloud cover at 1600 GMT on the analyzed days. There appears to be no correlation between severe weather days and the amount of morning cloudiness. Rather, the severe weather seems to occur on partially cloudy days. Therefore, it is possible to obtain many clear-column satellite radiances on most severe weather days. This allows an analysis of the environmental gradients prior to severe weather development later in the day.

Fig. 15 shows the structure functions for the same 10 days at 1600 GMT but for the radiances from VTPR channel 7. Channel 7 is affected mainly by moisture and to a lesser extent by lower tropospheric temperature. The same two days (29 and 31 May) again show large structure function increases with distance. However, three other days (20 May, and 4 and 8 June 1976) also have large structure values even down to 100 km. The first two of these days reported thunderstorm activity but no other severe weather. These observed gradients in moisture as detected by the structure functions are important to severe weather development, but for the days examined here only those days with large structure-function slopes for both VTPR channels 6 and 7 did report funnel clouds and hail. The remaining days had lower structure values and the clear, no activity day (18 May 1976) again had nearly the lowest structure values.

The structure functions for individual fields of satellite-derived 500 mb temperatures for the same days and times are shown in Fig. 16. These structure functions reflect temperature gradients in the upper troposphere. For 31 May 1976 the structure function reaches a maximum and decreases to near zero structure at 800 km. In the case of a one-dimensional gradient, this would indicate a temperature wave (cold tongue) with a width roughly equal to this distance in the region of study, as was confirmed by the 1200 GMT 500 mb synoptic temperature analysis (not shown). The other severe weather day (29 May) had the largest structure values beyond 700 km, indicating mainly a larger scale temperature gradient. A large north–south temperature gradient was the main feature on this day. Only an anisotropic structure-function analysis will allow independent determination of the component gradients.

The only other day that had structure-function values greater than the structure on the two severe storm days was 14 May 1976, That day had a cold cutoff low in the upper atmosphere at the 500 mb level. These structure functions, therefore, appear to reflect upper air features, but they do not show as great a distinction between severe and nonsevere days as do the radiances for channels 6 and 7. Upper air support does have an effect on summertime convective activity, but some important ingredients besides instability and a trigger mechanism are lower tropospheric temperature and

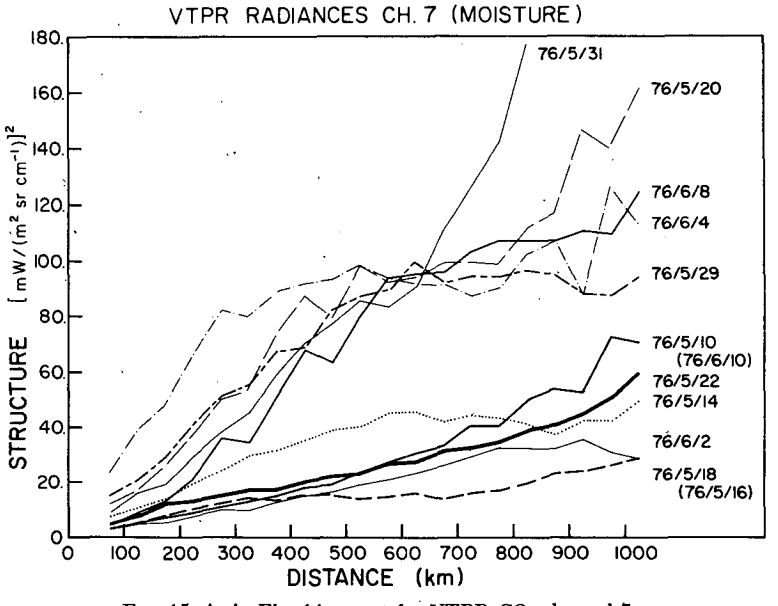

FIG. 15. As in Fig. 14 except for VTPR CO_2 channel 7.

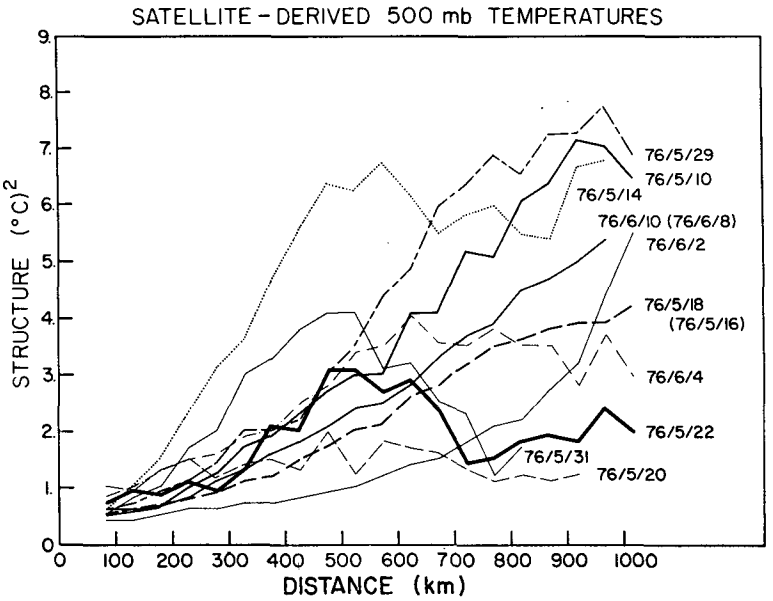

FIG. 16. Satellite-derived 500 mb temperature structure as a function of sounding separation distance for individual satellite passes at approximately 0900 CST on each day.

moisture gradients. These gradients are necessary for potential energy release in order to produce severe weather.

8. Independent analysis of the information content of satellite-derived temperature and moisture fields

Because the satellite sounder and rawinsonde are intrinsically different instruments, it is hard to compare them on an equal baisis. Structure-function analysis is one means of comparison which also provides an uncertainty analysis for each instrument. However, when measurements from the two instruments are compared, they each contain errors and neither can be said to be the correct or true value. Despite these differences, there still is some validity in a comparison. The comparison will not give the absolute accuracy of one instrument, but only its accuracy compared to another possibly equally inaccurate instrument. Such comparisons can only tell us if both instruments at least try to give us the same information.

The major differences between the satellite sounder and the rawinsonde are related to the vertical and horizontal averaging which takes place in the sensing of satellite temperatures. Bruce *et al.* (1977) used a structure-function analysis of rawinsonde temperatures to show how the difference between point rawinsonde temperature measurements and radiometric area (or volume) temperatures causes a large portion of the standard error usually associated with satellite-rawinsonde comparisons. Even for the point rawinsonde measurements taken within a simulated radiometric area at 100 km resolution, there arise rms differences of 1–1.4°C. Much greater differences exist if the measurements are not coincident in time.

Probably most of the remaining discrepancy between rawinsonde and satellite temperatures is due to systematic biases between the data sets, but this can only be determined by differencing techniques or some independent check. A simple correlation between satellite and rawinsonde values at supposedly coincident points was performed to check the gross features of the measurements from each instrument. No indication of systematic differences is made, only whether the two data sets are spatially correlated over the whole field.

a. Temperature analysis

To compare satellite and rawinsonde temperatures requires that the two measurements be colocated in space and time. The rawinsonde temperature measurement occurs at a point which moves horizontally as the rawinsonde balloon ascends. To avoid problems with the exact location of the rawinsonde, the closest satellite sounding positions were averaged to form one value for comparison. All satellite sounding center points within a 75 km radius of the rawinsonde launch site are used in the average. This average includes one to four satellite soundings depending on the position of the satellite and whether the soundings were cloud free. Correlations were than calculated for all paired satellite-rawindonde values, one for each rawinsonde location.

For the analysis of temperature, which varies on larger space and time scales than moisture, the rawinsondes used for comparison were the NWS synoptic network shown in Fig. 4. For these eight stations, soundings are available at 1200 GMT before the

TABLE 6. Temperature correlations.

Date	Number of satellite-NWS pairs	Satellite vs 1600 GMT interpolated NWS			1200 GMT NWS vs 0000 GMT NWS		
		300 mb	500 mb	700 mb	300 mb	500 mb	700 mb
(1976)							
10 May	4	0.84	0.97	0.48	0.88	0.78	0.78
12 May	0	—	cloudy	—	0.20	0.07	0.75
14 May	8	0.24	0.81	0.93	0.52	0.84	0.80
16 May	6	0.78	0.50	0.62	0.46	0.03	0.83
18 May	8	0.35	0.91	0.15	0.81	0.45	0.71
20 May	2	—	cloudy	—	0.65	0.40	0.05
22 May	4	0.93	0.34	0.62	0.21	0.12	0.87
29 May	4	0.81	0.89	0.75	0.77	0.41	0.95
31 May	5	0.62	0.76	0.87	0.73	−0.28	0.50
2 June	6	0.68	0.52	0.84	0.14	0.59	0.74
4 June	6	0.96	0.99	−0.29	0.88	0.53	0.67
6 June	1	—	cloudy	—	0.80	0.34	0.83
8 June	4	0.62	0.58	−0.19	0.73	0.75	0.62
10 June	6	0.83	0.96	0.59	0.57	0.36	0.72

satellite overpass (at approximately 1600 GMT) and at 0000 GMT after the pass. Because neither time period is close enough to the satellite pass, the two time periods were used to create linear time-interpolated rawinsonde temperature values at 1600 GMT for comparison.

The NSSL rawinsonde temperatures were not used for comparison with the satellite-derived temperatures because of the small-magnitude temperature gradients observed on many days. The mean gradient over 200 km as measured by either the satellite temperature structure or the NSSL temperature structure at 500 mb is ~1°C as shown in Fig. 12. Since the rms satellite uncertainty is 0.5°C, little if any signal in the mean would be present above the noise level within this distance. A much better set of rawinsondes for comparison would be a high-density network that extended more than 500 km. The only choice, however, was the NWS synoptic rawinsonde network. Although these soundings were not high-density, at least they covered an area where the mean gradient in 500 mb temperatures was ~2°C at 800 km. Smaller and larger mean gradients are observed at 300 and 700 mb, respectively, as shown in Fig. 8.

The results of the satellite-NWS temperature correlations are shown in the first four columns in Table 6. Correlations for temperatures at 300, 500 and 700 mb are listed for each of the 14 days along with the number of pairs of measurements. Three days were sufficiently cloudy around many of the rawinsonde sites to preclude any correlation analysis. Even on clear days a maximum of eight pairs of satellite-NWS temperature pairs were used in the correlation, so the correlations are not very significant unless correlations are high.

The last three columns in Table 6 give the correlations between the 1200 and 0000 GMT NWS rawinsonde temperatures at the same three levels. If these correlations are not large, then there was probably some significant temperature pattern which was changing or advecting through the area, and any attempt at a linear interpolation to obtain temperatures at 1600 GMT may or may not prove successful. Some of the lowest 1200–0000 GMT correlation values were probably responsible for the correspondingly low satellite-NWS correlations which used the 1600 interpolated rawinsonde temperatures. For example, the satellite-NWS correlations at 500 mb are fairly high except for 3–4 days. Correlations of 0.5 or below at 500 mb occurred on 16 and 22 May 1976. The reason for these poor correlations may be due to the questionable 1600 GMT interpolated values used for comparison as shown by the low 1200–0000 GMT correlations at 500 mb on these days.

The correlations for 300 mb temperatures are also higher than 0.5 except for two days (14 and 18 May). The first day may have failed for the same reason as the 500 mb temperature explained above, but the second day does not have a low 1200–000 GMT correlation at 300 mb. Not all poor satellite-NWS correlations are explained by poor 1600 GMT interpolated values, but this source of error cannot be dismissed. On the other hand, there seems to be a much worse correlation record for 700 mb temperatures, with some days even having a small negative correlation. Temperatures at 700 mb were the hardest to retrieve due to cloud and moisture problems as well as a surface temperature factor in the lowest tropospheric CO_2 channel weighting functions. Together these error sources cause the wide range of correlations at 700 mb as shown in Table 6. Since cloud problems have been mostly eliminated by the cloud, no-cloud threshold at 900 mb, the one remaining major source of error was due to unknown moisture effects on the temperature retrieval process, as was pointed out previously. Lower tropospheric temperature fields can only be retrieved with reasonable accuracy when the atmospheric

moisture content and distribution are better known, and this will only be attainable with a more active role of moisture in the retrieval process.

b. *Moisture analysis*

The correlation analysis for moisture utilized the NSSL mesoscale sounding network. The statistical correlation function analysis showed that moisture correlation decreases rapidly with distance. It is assumed that the correlation also decreases rapidly in time. Therefore, it would be unreasonable to try to linearly interpolate 1600 GMT moisture values for comparison with satellite moisture values. The NSSL soundings, however, occur on a small space scale and were launched at 1500 GMT (0900 CST), within 1 h of the satellite soundings. Again, only satellite soundings with no detectable clouds above 900 mb were used.

The correlations shown in Table 7 indicate good results on only four days (16 and 18 May, and 4 and 6 June 1976). The negative correlations are the desired products, since the moisture residuals are in theory negatively related to rawinsonde precipitable water (PW) values. Three days were too cloudy for a comparison and the remaining days had low or positive correlations. Many days suffered from a small number of pairs in the correlation. To a large extent, poor correlations can also be explained by the relatively high noise level of the radiance residuals for channel 7. The rms noise level determined from the structure function for the radiance residuals gave a value of 1.09 mW/(m^2 sr cm^{-1}) at 75 km separation. For comparison, the standard deviations for the moisture residuals for each day are listed in Table 7. The standard deviations of the PW values used in the correlation are also shown. This value is expressed as the percentage of the mean value, since the absolute magnitude of the PW does not affect the correlation results given.

The correlation results for three of the four successful days show both a standard deviation for moisture residuals greater than the rms noise level of 1.09 mW/(m^2 sr cm^{-1}) and a PW standard deviation $>11\%$. One successful day (16 May 1976) did not have large standard deviations and one other day (10 May 1976) should have provided a negative correlation according to these criteria. Thus the integrated moisture information obtained from the satellite as measured by this analysis is not always reliable. Moisture gradients generally occur on smaller space and time scales than those for temperature, but on this NSSL sounding scale the moisture gradients on many days were too small to be detected above the noise level of the moisture residuals. Only on three of the days with the largest gradients in precipitable water across the field, as measured by a large PW standard deviation, were these gradients detected.

The maximum separation distance between any two NSSL soundings was $\sim$200 km. It is possible that a slightly larger network of NSSL soundings would contain large enough moisture gradients on other days to make the moisture correlations meaningful. From the structure-function analysis in Fig. 9, a separation of 200 km should give a mean gradient in the moisture residuals of 2.6 mW/(m^2 sr cm^{-1}), well above the noise level since the slope of the structure function is rather steep at small separation distances. However, this large gradient does not occur at all places or at all times as we have seen here, just as larger gradients also occur on other days.

TABLE 7. Moisture correlations.

Date	Number of pairs	Correlation PW vs residual channel 7	Standard deviation: Residual channel 7 [mW/(m^2 sr cm^{-1})]	Standard deviation: Precipitable water (percent of mean)
(1976)				
10 May	5	0.08	1.36	18
12 May	0	—	cloudy	—
14 May	8	0.26	0.38	14
16 May	9	−0.88	0.93	7
18 May	9	−0.64	2.16	19
20 May	0	—	cloudy	—
22 May	4	0.49	0.42	5
29 May	2	—	cloudy	—
31 May	7	0.05	0.69	10
2 June	9	−0.10	1.04	7
4 June	6	−0.91	1.75	18
6 June	5	−0.65	1.56	12
8 June	9	−0.24	1.72	10
10 June	9	0.84	0.46	10

9. Summary and conclusions

Because of the increasing demand for mesoscale data for forecasting and computer simulation models, it is necessary to be able to extract and utilize the information content of these data. Satellites can supply large quantities of high-resolution measurements. However, only when used at full resolution and on small space scales will the full potential of high-resolution satellite data be realized. Structure-function analysis may provide a means for interpreting such information from different space (and time) scales and from different measurement systems. This will be especially necessary for using data from upcoming satellite sounders in geosynchronous orbit. It may not be necessary to obtain absolute values from the satellite. Information about the temperature and moisture gradients is relatively easy to obtain from high-resolution satellite data by using structure-function analysis.

The structure as a function of distance reflects the mean nondirectional gradient for the measured fields used in the analysis. Root mean square noise levels for the satellite radiances and satellite-derived temperatures were obtained by extrapolating the structure values to zero separation from the minimum pair-

separation distance of 75 km. These uncertainty values are, therefore, not based on any intercomparison of satellites and rawinsonde data. The radiance error of $\sim$0.25 mW/(m^2 sr cm^{-1}) for the noncloudy CO_2 channels other than channel 1 is equivalent to the design sensitivity of the VTPR instrument. Likewise, the rms noise level for temperatures at 300, 500 and 700 mb is $\sim$0.5°C which is a very reasonable value for satellite soundings. Note that this value is much less than standard error values of 1–3°C usually associated with satellite-rawinsonde comparisons. This indicates that satellite soundings are more valuable than some contemporary comparisons may imply. However, no measure of systematic biases are made, only the smaller relative noise level is determined. This is a measure of maximum capabilities to be expected from second generation satellite soundings of this type and resolution.

The structure and correlation functions for all available satellite-derived temperature data during the 1976 NSSL sounding period compared favorably to similar results for NSSL mesoscale soundings. The differences between the structure functions for satellite and conventional rawinsonde temperatures are mainly due to the inherent vertical averaging differences between the instruments. The correlation results on the one satellite-derived moisture value, however, did not prove equivalent to the correlation analysis of rawinsonde mixing ratios at either 500 or 700 mb. This satellite, therefore, does not provide the detailed moisture information available from mesoscale rawinsondes, especially in terms of vertical moisture distribution.

It is of special note that structure functions for satellite radiances detect relative strengths of lower tropospheric temperature and moisture gradients on individual NSSL days. The analysis of 14 days of VTPR radiances for channels 6 and 7 (low troposphere) appear to show a delineation between significant and no activity weather days on the basis of increased radiance structure with distance. This is accomplished without the help of conventional data and without the retrieval of temperatures from the satellite radiances. In similar manner, structure functions for satellite-derived 500 mb temperatures appear to reflect the existing upper air patterns on individual analysis days by means of the detected temperature gradients.

Correlations between satellite and rawinsonde data were used to test the information content of the satellite soundings. Temperatures at 300 and 500 mb were retrieved with reasonably high success, but lower tropospheric temperatures and moisture were not reliably determined. Both cloud and moisture problems caused the derived 700 mb temperatures to be uncorrelated with the interpolated temperatures from the NWS rawinsonde network. The analysis of the moisture information was also made difficult by the weak moisture gradients detected on many analysis days on the scale of the NSSL sounding network. Only the largest gradients were detected. In either case, interpretation of the results is limited by the small number of comparison points and the small number of days under analysis.

The present study used 1976 satellite data from the operational VTPR sounder. Improvements in quality, yet not in concept, can be anticipated when 1978–80 instrument data available from the TIROS-N sounder are examined in a similar manner. Especially important improvements in moisture detection should be made both in terms of moisture content and distribution.

Acknowledgments. Special thanks go to Dr. Stanley L. Barnes at NOAA Environmental Research Laboratories in Boulder for the results of the structure function and correlation function analyses on the 1976 NSSL mesoscale soundings. The calibrated VTPR radiances from NOAA 4 were provided by the Indirect Soundings Branch of NOAA/NESS in Washington, DC.

Support for this research was received from the Atmospheric Science Section, National Science Foundation, under Grant ATM76-21307 and the Colorado State University Computer Center.

REFERENCES

Barnes, S. L., and D. K. Lilly, 1975: Covariance analysis of severe storm environments. *Preprints Ninth Conf. Severe Local Storms*, Norman, Amer. Meteor. Soc., 301–306.

Bruce, R. E., L. D. Duncan and J. H. Pierluissi, 1977: Experimental study of the relationship between radiosonde temperatures and satellite-derived temperatures. *Mon. Wea. Rev.*, **105**, 493–496.

Conrath, B. J., 1972: Vertical resolution of temperature profiles obtained from remote radiation measurements. *J. Atmos. Sci.*, **29**, 1262–1271.

Duncan, L. D., 1977: Zenith angle variation of satellite thermal sounder measurements. R & D Tech. Rep. ECOM-5828, Atmos. Sci. Lab., White Sands Missile Range, 7 pp. [NTIS AD-A044-660/9GI].

Gandin, L. S., 1963: Objective analysis of meteorological fields. Translated from Russian, Israel Program for Scientific Translations, Jerusalem, 242 pp. [NTIS TT-65-50007].

Grody, N. C., and P. P. Pellegrino, 1977: Synoptic-scale studies using the Nimbus 6 scanning microwave spectrometer. *J. Appl. Meteor.*, **16**, 816–826.

Hillger, D. W., and T. H. Vonder Haar, 1977: Deriving mesoscale temperature and moisture fields from satellite radiance measurements over the United States. *J. Appl. Meteor.*, **16**, 715–726.

Kelly, G. A. M., G. A. Mills and W. L. Smith, 1978: Impact of Nimbus-6 temperature soundings on Australian region forecasts. *Bull. Amer. Meteor. Soc.*, **59**, 393–405.

Kreitzberg, C. W., 1976: Interactive applications of satellite observations and mesoscale numerical models. *Bull. Amer. Meteor. Soc.*, **57**, 679–685.

Lilly, D. K., Ed., 1975: Open SESAME, Severe environmental storms and mesoscale experiment. *Proc. Open Meeting*, Boulder, 499 pp. [Govt. Publ. Order No. C55.602:Sr8].

McMillin, L. M., D. Q. Wark, J. M. Siomkajlo, P. G. Abel, A. Werbowetzki, L. A. Lauritson, J. A. Pritchard, D. S. Crosby, H. M. Woolf, R. C. Luebbe, M. P. Weinreb, H. E. Fleming, F. E. Bittner and C. M. Hayden, 1973: Satellite infrared soundings from NOAA spacecraft. NOAA Tech. Rep. NESS 65, 112 pp. [NTIS COM-73-50936/6AS].

Petersen, R. A., and L. H. Horn, 1977: An evaluation of 500 mb height and geostrophic wind fields derived from Nimbus-6 soundings. *Bull. Amer. Meteor. Soc.*, **58**, 1195–1201.

Rodgers, C. D., 1976: The vertical resolution of remotely sounded temperature profiles with a priori statistics. *J. Atmos. Sci.*, **33**, 707–709.

Shaw, J. H., M. T. Chahine, C. B. Farmer, L. D. Kaplan, R. A. McClatchey and P. W. Schaper, 1970: Atmospheric and surface properties from spectral radiance observations in the 4.3 micron region. *J. Atmos. Sci.*, **27**, 773–780.

Thompson, O. E., J. K. Eom and J. R. Wagenhofer, 1976: On the resolution of temperature profile finestructure by the NOAA satellite vertical temperature profile radiometer. *Mon. Wea. Rev.*, **104**, 117–126.

Tracton, M. S., and R. D. McPherson, 1977: On the impact of radiometric sounding data upon operational numerical weather prediction at NMC. *Bull. Amer. Meteor. Soc.*, **58**, 1201–1209.

Weinreb, M. P., 1977: Sensitivity of satellite retrievals of temperature to errors in estimates of tropospheric water vapor. *J. Appl. Meteor.*, **16**, 605–613.